LinkRbrain: Multi-scale data integrator of the brain

Salma Mesmoudi, Mathieu Rodic, Claudia Cioli, Jean-Philippe Cointet, Tal Yarkoni, Yves Burnod

LinkRbrain: multi-scale data integrator of the brain.

Salma Mesmoudi[a,*], Mathieu Rodic[a], Claudia Cioli[b], Jean-Philippe Cointet[c], Tal Yarkoni[d], Yves Burnod[b]

[a] *Sorbonnes university Paris 1, MATRICE Project, ISC-PIF, 75013 Paris, France.*
[b] *Sorbonne University, UPMC Univ Paris 06, Laboratoire Imagerie Biomedicale, ISC-PIF, 75013 Paris, France.*
[c] *INRA-SenS, IFRIS / UPEM, ISC-PIF, 75013 Paris, France.*
[d] *University of Texas at Austin. Department of Psychology*

Abstract

Background: LinkRbrain is an open-access web platform for multi-scale data integration and visualization of human brain data. This platform integrates anatomical, functional, and genetic knowledge produced by the scientific community.
New Method: The linkRbrain platform has two major components: 1) a data aggregation component that integrates multiple open databases into a single platform with a unified representation; and 2) a website that provides fast multi-scale integration and visualization of these data and makes the results immediately available.
Results: LinkRbrain allows users to visualize functional networks or/and genetic expression over a standard brain template (MNI152). Interrelationships between these components based on topographical overlap are displayed using relational graphs. Moreover, linkRbrain enables comparison of new experimental results with previous published works.
Comparison with Existing Methods: Previous tools and studies illustrate the opportunities of data mining across multiple tiers of neuroscience and genetic information. However, a global systematic approach is still missing to gather cognitive, topographical, and genetic knowledge in a common framework in order to facilitate their visualization, comparison, and integration.
Conclusions LinkRbrain is an efficient open-access tool that affords an in-

*Corresponding author
Email address: salma.mesmoudi@gmail.com (Salma Mesmoudi)

tegrative understanding of human brain function.

Keywords: platform, multi-scale, anatomo-functional, genetics, integrative, complex systems, open databases
2014 MSC: 00-01, 99-00

1. Introduction

Sensorimotor and cognitive processing in humans is dependent on the anatomical and functional organization of the brain [Fox et al. (2005); Laird et al. (2011); Mesmoudi et al. (2013)]. Numerous studies have been conducted that focus on a single level of brain organization such as the anatomical [Catani et al. (2013)], the functional [Blumensath et al. (2013)] or the genetic level [Hawrylycz et al. (2012)]. However to really understand the emergence of human cognition, it is necessary to investigate the relationships between these different scales and study the brain as a complex system. The main challenge is thus the integration of available multi-scale knowledge about brain function. Previous studies have tried to link the expression of certain genes with specific cognitive functions [Zeng et al. (2012); Grange et al. (2014); Hawrylycz et al. (2012); Glahn et al. (2010)]. In parallel, fMRI studies have related brain hemodynamic activity to cognitive and sensorimotor function. Manual and automated meta-analysis of large databases of neuroscientific papers have integrated results into synthetic representations (BrainMap [Laird et al. (2005)] and NeuroSynth [Yarkoni et al. (2011)], respectively). These methods are based on extraction of fMRI activation peaks (i.e coordinates) as reported in published articles. They support construction of probabilistic maps of specific cognitive functions.

To visualize and analyze the complex convolutions of the cerebral cortex, the Caret platform provides a powerful approach to quantitatively represent both the consistency and variability in the pattern of convolutions and functional activation from any given task. This tool also allows supports comparisons across species and evaluation of candidate homologies between cortical areas or functionally delineated regions [Van Essen (2004)].

Brainscanner was developed in order to analyze abstracts from scientific papers published in peer-reviewed journals. It measures lexical associations between neuroscientific concepts, then extracts relationships between brain structures, functions, and diseases [Voytek and Voytek (2010)]. Other tools such as the Genetic Association Database (GAD) [Becker et al. (2004)],

GeneCard [Safran et al. (2010)], and GeneBank [Benson et al. (2005)] collect, standardize, and archive valuable genetic information. The GeneMANIA tool can be used to find other genes that are related to a set of input genes, based on a very large set of functional association data such as protein and genetic interactions, pathways, co-expression, co-localization and protein domain similarity [Warde-Farley et al. (2010)].

Recently, the Allen Institute for Brain Science (ABI) released an open access database called the "Allen Human Brain Atlas" [Jones et al. (2009)] that contains expression data for 21,000 different genes across 1000 brain regions.

In addition, the Neuroscience Information Framework (NIF) [Akil and Martone (2011)] provides a unified portal to several neuroscience databases, facilitating access to existing knowledge from neuroimaging, neuroanatomy, cognitive, and genetics databases.

These tools illustrate the opportunities for data mining across multiple sources of neuroscience and genetic information. However, the field is currently lacking a global systematic approach for gathering cognitive, topographical, and genetic knowledge in a common framework that can facilitate visualization, comparison, and integration.

In order to take on the challenge of integrating cognitive, genetic, and anatomical knowledge about brain function, we developed the *linkRbrain* platform (*www.linkrbrain.org*). This platform (1) accumulates information from several databases, and (2) integrates these multi-scale data into a common framework so that every point in the brain is characterized by a cognitive profile, a gene expression profile, and a neuroanatomical label. Thus, *linkRbrain* systematically links: (1) a set of activation peaks over the brain to a set of cognitive labels; (2) a genetic expression profile to a set of cognitive labels; and (3) a set of cognitive labels or genetic expression profile to neuroanatomical labels.

The *linkRbrain* platform provides brain mapping and relational graphs comprising current available information on brain activity, genetic expression and cognitive functions. This integrative platform is available to the whole community, through an open collaborative website.

2. Data sources

Functional MRI data. LinkRbrain relies on the database of activation peaks generated by the Neurosynth framework [Yarkoni et al. (2010)] [1]. The version of the database used in *linkRbrain* contains 194,387 activation peaks automatically extracted from over 5000 published neuroimaging papers, with roughly 140,974 coordinates correctly labeled in Talairach or MNI [Talairach and Tournoux (1993); Evan et al. (1993)].

Article abstracts. In order to extract the terms used by authors to describe cognitive tasks in a bottom-up manner, we used the abstracts and titles of over 5000 neuroimaging articles contained in the Neurosynth database.

Gene expression data. The Allen Human Brain Atlas (ABA) [Jones et al. (2009)] produced by the Allen Brain Institute (ABI) provides microarray expression profiles of almost every gene in the human genome at hundreds of locations in the brain. Two complete postmortem brains (H0351.2001 and H0351.2002) are available. Genetic profiles of the two brains are highly compatible [Hawrylycz et al. (2012)]. *LinkRbrain* used the H0351.2001 ABA, which reports the genetic profiles for a set of 947 samples, representing the structures within the human brain in approximate proportion to the volumetric representation of each cortical, subcortical, cerebellar, and brain stem structure. This first version of *linkRbrain* supports visualization of about 21,000 genes expression profiles (as studied in [Hawrylycz et al. (2012)]) across the complete set of 947 brain regions.

The H0351.2001 ABA dataset contains about 451 cortical and 496 subcortical regions. To avoid driving results that could be induced by the oversampling of the subcortical structure, the first version of *linkRbrain* focuses exclusively on human cortical organization. Hence, the graphs used to quantify gene/cognition overlap and gene/gene overlap take into account only the cortical samples (451 regions).

Neuroanatomical data. We used the *3D Talairach Atlas*[Lancaster et al. (2000)] to label neuroanatomical structures. This atlas was created from the reference images using resampling following the x and y axis and nearest neighbor interpolation in the z direction. The 3D Talairach Atlas is available as

[1] available at *(http://neurosynth.org)*

a *NIFTI* image "Talairach.nii", where every voxel refers to one of the area labels.

3. Methods

3.1. Text mining

Two types of relations link the sensorimotor/cognitive tasks. First, lexical relations can be directly extracted from the text of articles, thereby providing an overview of the relations between cognitive domains as conceptualized by the scientific community as a whole. Second, topographical relations can be estimated by quantifying the spatial overlap between task-related activations for different functions. In this work, we focus on topographical relations between cognitive networks, genetic expression profiles, and neuroanatomical structures.

Cognitive task labels. We used the lexical extraction capabilities of the CorText platform to identify a set of pertinent terms. Text processing involves both grammatical[2] and statistical [Kageura (1996); Frantzi and Ananiadou (2000)] phases to automatically extract candidate n-grams (also called multitems)[3]. We analyzed the textual content found in titles and abstracts of the 5000 papers within Neurosynth (corpus). The most pertinent noun phrases in our corpus were then curated by a neuroscientist who manually selected the 300 most frequent sensorimotor/cognitive tasks (e.g. *spatial working memory*, *emotional facial expressions*)

Linking activation peaks and task labels. Neurosynth data and software [4] were used to generate a meta-analytic reverse inference map [Yarkoni et al. (2011); Poldrack (2006)] for each of the previously extracted n-grams. This map quantifies the degree to which each brain region is preferentially activated in studies tagged with a particular sensorimotor/cognitive task label.

[2]The POS-tagging step assigns grammatical tags to each word, which are then exploited to find noun phrases (in the "chunking" step). The NLTK python library [Bird et al. (2009)] was used to perform these tasks.

[3]Further information about textual processing, is available in the CorText documentation http://docs.cortext.net/lexical-extraction.

[4]available at *(http://github.com/neurosynth)*

3.2. From probes to expression of genes

Genetic expression profiles of the H0351.2001 Atlas were published by ABI as a matrix of $58000 probes \times 947 regions$ of the brain, and includes a list of correspondences between probes and genes [Jones et al. (2009)]. The final expression profile of every gene was computed by averaging the corresponding probes.

3.3. Topographical distances

The topographical overlap among cognitive activations, between cognitive activations and gene expression regions, or between cognitive activations/gene expression regions and anatomical structure of brain, is expressed as a distance based on a correlation metric. Each network (corresponding to a cognitive task, gene expression region, or anatomical structures of brain) is a set of points or *nodes*. Let two nodes (sets of weighted points) A and B:

$A = \{(M_i, \mu_i) | i \in [\![1, m]\!]\}$

$B = \{(N_j, \nu_j) | j \in [\![1, n]\!]\}$,

where μ_i and ν_j are the weights of M_i and N_j respectively.

The weights express statistical or genetic expressions values related to the activation peaks or cortical regions respectively.

The correlation score (cor) between the nodes A and B was defined by the formula:

$$cor(A, B) = \sum_{d(M_i, N_j) \leqslant r} \mu_i . \nu_j \frac{d(M_i, N_j)}{r}, \tag{1}$$

where r is the reference radius (10 mm in this case, consistent with the meta-analysis), and $d(M_i, N_j)$ is the distance between two points M_i and N_j.

The overlap between the two nodes A and B, was obtained by normalizing the correlation score with their autocorrelation. This overlap was based on the RV coefficient [Robert and Escoufier (1976)]:

$$s(A, B) = \frac{cor(A, B)}{\sqrt{cor(A, A).cor(B, B)}} \tag{2}$$

3.4. Visualization

All the activation peaks extracted from the literature [Yarkoni et al. (2010, 2011)], the gene expressions regions [Jones et al. (2009)], or anatomical structures of brain [Lancaster et al. (2000)]are plotted on a 3D and 2D

reconstructed brain from the T1- weighted MNI152[Evan et al. (1993)]. 3D visualization allows a global localization of studied networks or regions of brain, while 2D visualization allows more precise location of various anatomical structures of the brain.

Visualization of activation peaks. We use the MAP inference procedure to generate sensorimotor/cognitive networks from the activation peaks[Yarkoni et al. (2010)]. To better illustrate the spatial distribution and overlapping, only one color was assigned to each network. Every task can be represented in two different ways: as spheres, or as a continuous surface.

Fig.1 illustrates the spatial distribution of the networks involved in a sensorimotor transformation relevant to speech: the relation between a sound and the motor production of this sound by speech. The observation of this figure suggests a relation between the networks specialized in syllable production, sensory tone processing, and motor control of the lips.

Visualization of expression genes regions. For each gene, we identified 451 regions of cortical and 496 subcortical regions of gene expression. In this version of *linkRbrain*, we focused on the cortical region to evaluate the overlap between task-based networks and genetic expression profiles. Plane visualization is anyway available for all the 947 regions that cover the cortical and subcortical brain regions. The expression of each of the 21,000 genes is represented by spheres located at each of the 947 brain samples; the diameter of each sphere is proportional to the intensity of expression of the given gene at this position in the brain (see Fig.2).

Visualization of user results. LinkRbrain users can visualize and correlate their neuroimaging results with the sensorimotor/cognitive networks, neuroanatomical regions, or genetic expression regions by loading a *NIFTI* file or MNI coordinates (using *NIFTI files*, *input coordinate*, or *text files* option). Moreover, by using the *input coordinate* or *text file* options, the user can (1) quickly and easily compare the expression among several genes by mapping only the cortex regions where they are the most expressed, and (2) upload her genetic results or a specific probe from the ABA dataset to correlate it with sensorimotor/cognitive networks.

Graph-based visualization of correlations. The topographical overlaps (i.e. correlations) between selected task(s), gene(s), or neuroanatomical regions

(current node) and the other cognitive tasks, genes, or neuroanatomical regions (nodes) can be represented as a graph. The graph is computed using the force-directed layout algorithm [Fruchterman and Reingold (1991)]. Fig.4 shows two types of links: (1) Colored links connect the current node to another node and reveal that an overlap exists between these two nodes; (2) Grey links express the overlap between the other nodes without involving the current node. The thickness of the link is proportional to the magnitude of the correlation (overlap).

Visualization of correlations with identified neuroanatomical structures. To identify the regions involved in cognitive activation or genetic expression regions, *linkRbrain* quantified the overlap (i.e. correlations) between this input and the structures of brain identified in the *Talairach* atlas. These results can be represented as colored regions in the brain, or a graph with cognitive activation or genetic expression regions (see Fig.5).

4. *LinkRbrain* as a multi-scale, integrative explorer

4.1. From cognitive functions to functional-anatomical architecture

To separately assess the performance of *linkRbrain* as an exploratory tool at the cognitive and the topographical scales, and as an integrated multi-scale tool, we used the example of the model called "the dual intertwined ring architecture" [Mesmoudi et al. (2013)]. This model originated from a systematic analysis of anatomical, resting-s tate (RSN), and task based networks (TBN). According to this model, the human cerebral cortex comprises two large ensembles shaped like two rings. The first ring, called the Visual-Sensorimotor- Auditory ring (VSA ring), comprises visual, auditory, somatosensory and motor cortices, including intermediate bimodal regions. The second ring, called the Parieto-Temporo-Frontal ring (PTF ring), comprises parietal, temporal, and frontal regions. The VSA ring is continuous and forms a circle around the parietal areas BA 39 and 40, whereas the PTF ring, which is not fully continuous over the cortical mantle, is closed by the long-range association fiber tracts (longitudinal parieto-frontal, arcuate, uncinate, and cingulum) that complete the intertwining. The two rings share a set of common regions mostly localized along the precentral, intraparietal, and superior temporal sulci.

Based on the overlap between the resting state networks and different areas and cortices, we can infer that the first ring (VSA ring) links various

sources of auditory, visual and somatomotor information together and to control actual behavior. These interactions are important, not only within each modality, but also for all of their bimodal interactions: between visual and motor (e.g., grasping, reaching, imitation), between auditory and somatomotor information (e.g., recognizing and producing phonemes) and between auditory and visual information (important for communication). To illustrate these functional interactions, we used *linkRbrain* to build the VSA ring by plotting on the brain the task based networks (TBN) corresponding to these modalities (visual, auditory, and motor) and bimodal interactions (motor-visual, visual-auditory, etc). As shown in Fig.6, we plot in blue the activations corresponding to: motor function, pictures, hand gestures, limb, somatomotor stimulation, auditory, etc. These networks are activated when we directly stimulated the visual, motor and auditory cortices. In addition, to obtain the bimodal interactions, we plot activations corresponding to speech, oculomotor, etc.

The PTF ring (in red) interfaces systems dedicated to higher cognitive functions with systems dedicated to emotions, biological needs and rhythms. In Fig.6 we showed that the PTF ring (in red) was reconstructed functionally by plotting the activations peaks corresponding to functions such as recollection, autobiographical memory, semantic memory, working memory, episodic memory, etc.

4.2. From genetic expression to cognitive functions

As explained in the *Methods section*, the *linkRbrain* platform computes the topographical overlap on the brain between different cognitive activations, gene expression regions, or between cognitive activations and gene expression regions. This topographical overlap is based on a correlation metric, and is represented by *linkRbrain* as a graph of topographical correlations. To illustrate these correlations, we compare the gene expression profiles of the Oxytocin receptor (OXTR) [Grillon et al. (2013); Hurlemann et al. (2010)], and the Dopamine D5 Receptor (DRD5) [Lak et al. (2014); Sunahara et al. (1991)](see Fig.7). Results show large overlaps, with an important difference: DRD5 is more highly expressed in the anterior cingutate cortex , and OXTR is more highly expressed in the medial anterior temporal pole. To compare the differential spatial correlations (overlap) with cognitive tasks, *linkRbrain* provides the graphs of topographical similarities. This graph is obtained from the correlation between regions of expression of the OXTR and DRD5 genes and all the activations corresponding to the 300 cognitives

tasks extracted from the 5000 neuro-cognitive papers. We see that both regions of gene expression are related to Reward, but OXTR expression is more strongly associated with overlapping emotional networks, and in particular facial expression (important for social interation), while DRD5 is more related to autobiographical memory, self, and interoceptive awareness. These results obtained from the overlap between genetic expressions and cognitive networks, are confirmed by the literature. In fact, several studies suggest a modulatory role of oxytocin on amygdala responses to facial expressions [Domes et al. (2007); Lischke et al. (2012)] (see Fig.4). Conversely, other studies implicate dopaminergic pathways in regulation of neuronal systems associated with reward sensitivity, self-control,and interoceptive awareness [Volkow et al. (2013)].

5. *LinkRbrain* as comparator of brain networks of cognitive functions

The cognitive functions "speech" and "sentences" are considered as two distinct functions. The "speech" function is related to word production, syllables, and/or vowels production and/or recognition [Scott et al. (2000); Narain et al. (2003)], while the "sentences" function is concerned with the meaning of sequences of words. This function is related to language comprehension and memory [Harris et al. (2014); Uchiyama et al. (2012)]. Thus, all of these cognitive differences should be topographically reflected. In Fig.8, by plotting the networks corresponding to the functions "speech" and "sentences"(colored in purple and magenta respectively), we notice: (1) the "V" shape that characterize these two functions, with a temporal and a frontal component; and (2) despite the proximity of these functions, their topographies are clearly different.

In the corresponding graph generated by *linkRbrain* two sets of the interactions with the other cognitives functions emerge. The first one is related to the "speech" functions (connected to the purple node) with functions such as: vowels, syllables production, etc.

The second set is related to the "sentences" function (connected to the magenta node) and represents cognitive functions that topographically overlap with "sentences", such as: speech comprehension, language processing, etc.

6. *linkRbrain* as a comparator of user results with the literature

Laird et al. reconstructed 20 intrinsic connectivity networks (ICN) from the BrainMap database which archived the peak coordinates and metadata associated with 8637 functional brain imaging experiments[Laird et al. (2011)]. These experiments were extracted from 1840 publications that reported 69,481 activation locations across 31,724 subjects. The masks of these 20 ICN [5]. Based on [Laird et al. (2011)], we used the ICN7 as example which include dorsolateral prefrontal (BA 46) and posterior parietal cortices (BA 7). ICN7 involve visuospatial processing and reasoning, with a strong weighting for tasks such as the mental rotation, and counting or calculation.

Based on correlations between the ICN7 image and each cognitive network in the *linkRbrain* database (see methods section), we produced a proximity graph. According to the graph of topographical proximities (see Fig.9), the volume analyzed corresponds to cognitive functions such as oculomotor, visuospatial working memory, saccades, anti-saccades, arithmetic operation and mental calculation. Theses functions extracted by *linkRbrain* are quite similar with those described in [Laird et al. (2011)].

7. Conclusion

The number of shared fMRI databases and genetic studies is continuously increasing thanks to the collective efforts of the scientific community. In this work we exploited several new open access databases, extending their value by integrating them in a common framework: a multi-scale data integrator. In fact, with the *linkRbrain* platform we can: (1) integrate anatomical, functional, and genetic knowledge, (2) visualize and compare functional networks and/or genetic expression, and (3) make sense of new experimental results produced by the community by comparing them with previously published work. In the future, we will extend the *linkRbrain* platform to include: (1) the new NeuroSynth database with 9721 studies, (2) fiber tracts data, to extend the present integration of multiscale data, and (3) new data coming from the community of users to extend and improve the existing database of cognitive task networks.

Acknowledgements

[5] available from *brainmap.org/icns*

We would like to thank the Allen Institute for Brain Sciences for sharing their human brain genetic expression data. We also thank the National Agency for research (ANR "Investissement Avenir") and the MATRICE project (especially Dr. D. Peschansky) for funding this work.

References

Akil, H., Martone, M E. andVan Essen, D. C., 2011. Challenges and opportunities in mining neuroscience data. Science 331 (6018), 708–712.

Becker, K., Barnes, K., Bright, T., Wang, S., 2004. The genetic association database. Nature Genetics 36, 431 – 432.

Benson, D., Karsch-Mizrachi, I., Lipman, D., Ostell, J., Wheeler, D., 2005. Genbanck. Nucleic Acids Res.

Bird, S., Klein, E., Loper, E., 2009. Natural language processing with python. oreilly media inc.

Blumensath, T., Jbabdi, S., Glasser, M., Van Essen, D., Ugurbil, K., Behrens, T., Smith, S., 2013. Spatially constrained hierarchical parcellation of the brain with resting-state fmri. Neuroimage 76, 313–24.

Catani, M., de Schotten, M. T., Slater, D., Dell'Acqua, F., 2013. Connectomic approaches before the connectome. NeuroImage 80, 2–13.

Domes, G., Heinrichs, M., Glscher, J., Bchel, C., Braus, D., Herpertz, S., 2007. Oxytocin attenuates amygdala responses to emotional faces regardless of valence. BIOL PSYCHIATRY 62, 11871190.

Evan, A., Collins, D., Mills, S., Brown, D., Kelly, R., , Peters, T., 1993. 3d statistical neuroanatomical models from 305 mri volumes,. Proc. IEEE-Nuclear Science Symposium and Medical Imaging Conference,, 18131817.

Fox, M. D., Snyder, A. Z., Vincent, J. L., Corbetta, M., Van Essen, D. C., Raichle, M. E., 2005. The human brain is intrinsically organized into dynamic, anticorrelated functional networks. PNAS 102(27), 9673–9678.

Frantzi, K., Ananiadou, S., 2000. Automatic recognition of multi-word terms: the c-value/nc-value method. international journal on digital libraries.

Fruchterman, T. M. J., Reingold, E., 1991. Graph drawing by force-directed placement. Software-Practice and Experience. 21 (11), 1129–1164.

Glahn, D., Winkler, A., Kochunov, P., Almasy, L., Duggirala, R., Carless, M., Curran, J., Olvera, R., Laird, A., Smith, S., Beckmann, C., Fox, P., Blangero, J., 2010. Genetic control over the resting brain. Proc Natl Acad Sci U S A 107 (3), 1223–8.

Grange, P., Bohland, J., Hawrylycz, M., Okaty, B., Mitrah, P., 2014. Cell-typebased model explaining coexpression patterns of genes in the brain. PNAS.

Grillon, C., Krimsky, M., Charney, D., Vytal, K., Ernst, M., Cornwell, B., 2013. Oxytocin increases anxiety to unpredictable threat. Mol. Psychiatry 18 (9), 95860.

Harris, L., Olson, A., Humphreys, G., 2014. The link between stm and sentence comprehension: A neuropsychological rehabilitation study. Neuropsychol Rehabil. 5, 678–720.

Hawrylycz, M., Lein, E., Guillozet-Bongaarts, A., Shen, E., al., 2012. An anatomically comprehensive atlas of the adult human brain transcriptome. Nature 489, 391399.

Hurlemann, R., Patin, A., Onur, O., Cohen, M., Baumgartner, T., Metzler, S., Dziobek, I., Gallinat, J., Wagner, M., Maier, W., Kendrick, K., 2010. Oxytocin enhances amygdala-dependent, socially reinforced learning and emotional empathy in humans. J. Neurosci. 30 (14), 49995007.

Jones, A., Overly, C., Sunkin, S., 2009. The allen brain atlas: 5 years and beyond. Nat Rev Neurosci 10, 821828.

Kageura, K., 1996. Methods of automatic term recognition: A review. Terminology 3 (2), 259–289.

Laird, A., Lancaster, J., Fox, P., 2005. Brainmap: The social evolution of a functional neuroimaging database. Neuroinformatics 3, 65–78.

Laird, A. R., Fox, P. M., Eickhoff, S. B., Turner, J. A., Ray, K. L., McKay, D. R., Glahn, D. C., Beckmann, C. F., Smith, S. M., Fox, P. s., 2011. Behavioral interpretations of intrinsic connectivity networks. J Cogn Neurosci. 23(12), 4022–4037.

Lak, A., Stauffer, W., Schultz, W., 2014. Dopamine prediction error responses integrate subjective value from different reward dimensions. Proc Natl Acad Sci U S A 111 (6), 2343–8.

Lancaster, J., Woldorff, M., Parsons, L., Liotti, M., Freitas, C., Rainey, L., Kochunov, P., Nickerson, D., Mikiten, S., Fox, P., 2000. Automated talairach atlas labels for functional brain mapping. Human Brain Mapping 10, 120131.

Lischke, A., Gamer, M., Berger, C. andGrossmann, A., Hauenstein, K., Heinrichs, M., Herpertz, S., G, D., 2012. Oxytocin increases amygdala reactivity to threatening scenes in females. Psychoneuroendocrinology 37, 14311438.

Mesmoudi, S., Perlbarg, V., Rudrauf, D., Messe, A., Pinsard, B., al., 2013. Resting state networks' corticotopy: the dual intertwined rings architecture. PLoS One.

Narain, C., Scott, S., Wise, R., Rosen, S., Leff, A., Iversen, S., Matthews, P., 2003. Defining a left-lateralized response specific to intelligible speech using fmri. Cereb Cortex. 12, 1362–8.

Poldrack, R., 2006. Can cognitive processes be inferred from neuroimaging data? Trends in Cognitive Sciences 10 (2), 5963.

Robert, P., Escoufier, Y., 1976. A unifying tool for linear multivariate statistical methods: The rv-coefficient. Applied Statistics 25 (3), 257265.

Safran, M., Dalah, I., Alexander, J., Rosen, N., Iny Stein, T., Shmoish, M., Nativ, N., Bahir, I., Doniger, T., Krug, H., Sirota-Madi, A., Olender, T., Golan, Y., Stelzer, G., Harel, A., Lancet, D., 2010. Genecards version 3: the human gene integrator. Database.

Scott, S., Blank, C., Rosen, S., Wise, R., 2000. Identification of a pathway for intelligible speech in the left temporal lobe. Brain., 2400–6.

Sunahara, R., Guan, H., O'Dowd, B., al., 1991. Cloning of the gene for a human dopamine d5 receptor with higher affinity for dopamine than d1. Nature 350 (6319), 614619.

Talairach, J., Tournoux, P., 1993. Referentially oriented cerebral mri anatomy: An atlas of stereotaxic anatomical correlations for gray and white matter. Thieme Medical Publishers, New York.

Uchiyama, H., Saito, D., Tanabe, H., Harada, T., Seki, A., Ohno, K., Koeda, T., Sadato, N., 2012. Distinction between the literal and intended meanings of sentences: a functional magnetic resonance imaging study of metaphor and sarcasm. Cortex. 48 (5), 563–83.

Van Essen, D., 2004. Surface-based approaches to spatial localization and registration in primate cerebral cortex. NeuroImage 23, S97S107.

Volkow, N., Wang, G., Tomasi, D., Baler, R., 2013. Obesity and addiction: neurobiological overlaps. Obes Rev. 14 (1), 2–18.

Voytek, J., Voytek, B., 2010. Automated cognome construction and semi-automated hypothesis generation. Journal of Neuroscience Methods.

Warde-Farley, D., Donaldson, S., Comes, O., Zuberi, K., Badrawi, R., Chao, P., Franz, M., Grouios, C., Kazi, F., Lopes, C., Maitland, A., Mostafavi, S., Montojo, J., Shao, Q., Wright, G., Bader, G., Morris, Q., 2010. The genemania prediction server: biological network integration for gene prioritization and predicting gene function. Nucleic Acids Res. 38, W214W220.

Yarkoni, T., Poldrack, R., Nichols, T., Van Essen, D., Wager, T., 2011. Large-scale automated synthesis of human functional neuroimaging data.. Nat Methods. 8, 66570.

Yarkoni, T., Poldrack, R. A., Van Essen, D. C., Wager, T. D., 2010. Cognitive neuroscience 2. 0: building a cumulative science of human brain function.. Trends Cogn Sci. 14, 48996.

Zeng, H., Shen, E., Hohmann, J., Oh, S., Bernard, A., al., 2012. Large-scale cellular-resolution gene profiling in human neocortex reveals species-specific molecular signatures. Cell 149, 48396.

Figure legends

Figure 1: Mapping of the networks corresponding to the cognitive functions "syllables production", "pure tone" and "lips movement" in blue, red, and green respectively. On the right side we represent the activated regions by spheres, whereas on the left side we display these networks as a continuous surface.

Figure 2: 3D and 2D Mapping of the expression profile across the 947 brain regions for the Microtubule-associated Protein Tau (MAPT) gene. Each region is represented by a sphere whose diameter is proportional to the expression intensity at the specific region.

Figure 3: 3D and 2D Mapping of the regions of maximal expression for Microtubule-associated protein tau (MAPT) and Myelin basic protein (MBP) genes. Each region is represented by a sphere colored in blue or magenta to indicate MAPT or MBP expression respectively.

Figure 4: 2D mapping of the cognitive network "facial expression" in green. The corresponding graph shows the neuroanatomical regions involved in this network (overlap). In the bottom, 2D mapping of the the neuroanatomaical region called "Amygdala" in blue. The corresponding graph shows the sensorimotor/cognitve task-based networks that are localized in this region.

Figure 5: The graph shows the topographical similarities (overlap) between speech function (nodes in in magenta) and the 300 cognitive tasks. Only the most highly correlated tasks (25) are represented. The magenta links connect speech network with similar tasks. The gray links connect tasks with each others.

Figure 6: Mapping of the cognitive and sensorimotor functions related to the VSA ring (in blue), and some cognitive functions that reconstruct the PTF ring (in red). The corresponding graph shows these functions and confirm the topographical similarities (overlap) between VSA/PTF (in blue/red respectively) and the 300 tasks. The blue/red links connect VSA/PTF rings (respectively) with similar tasks. The gray links connect tasks with each other.

Figure 7: Mapping of the regions where the genes coding for oxytocin receptor (OXTR) and dopamine receptor D5 (DRD5) (in blue and red respectively) are the most expressed. the regions in purple represent the overlap between the two gene expressions. The corresponding graph shows the sensorimotor/cognitives task-based networks that are localized in the same regions where the genes OXTR and DRD5 are most strongly expressed. Red links connect the DRD5 expressions with the topographically nearest tasks, whereas the blue links connect the OXTR expressions with the topographically nearest tasks. The gray links connect tasks with each other on the basis of their topographical overlaps.

Figure 8: Mapping of the networks corresponding to the cognitive functions "speech" and "sentences" in purple and magenta respectively. The corresponding graph shows the topographical similarities (overlap) between the "speech" and "sentences" functions (respectively in purple and magenta) and the 300 cognitives tasks. The "purple/magenta" links connect "speech/sentences" networks (respectivelly) with similar tasks. The gray links connect tasks with each other.

Figure 9: The graph shows the topographical similarities (overlap) between the ICN7 network (colored nodes) and the 300 cognitive tasks. The colored links connect ICN7 network with similar tasks. The gray links connect the cognitive tasks with each other.

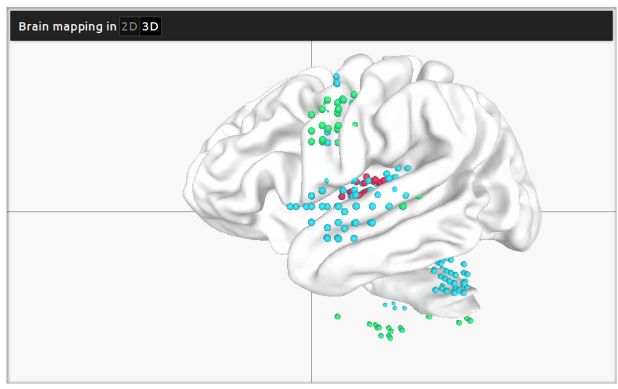
Brain mapping in 2D 3D

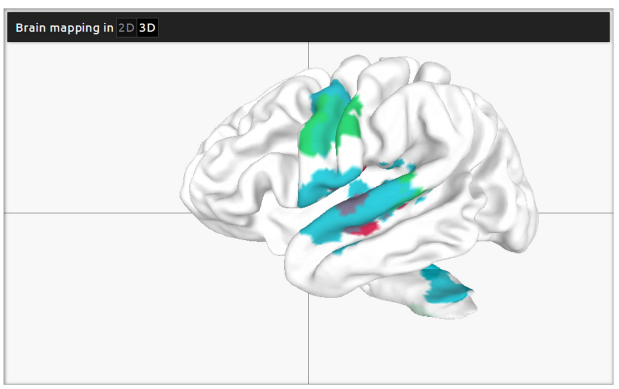
Brain mapping in 2D 3D

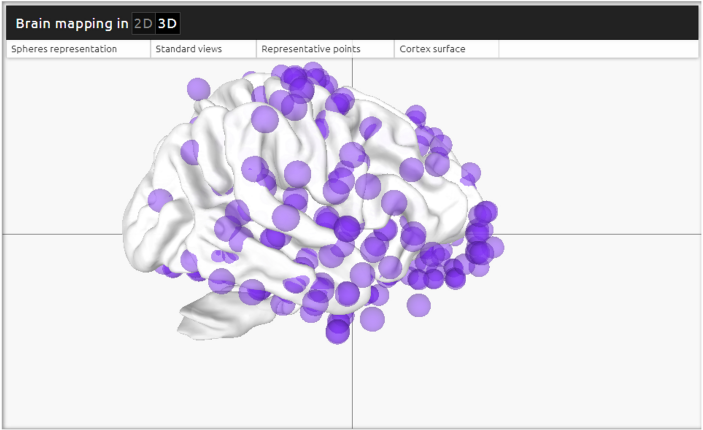
Brain mapping in 2D 3D
Spheres representation
Standard views
Representative points
Cortex surface

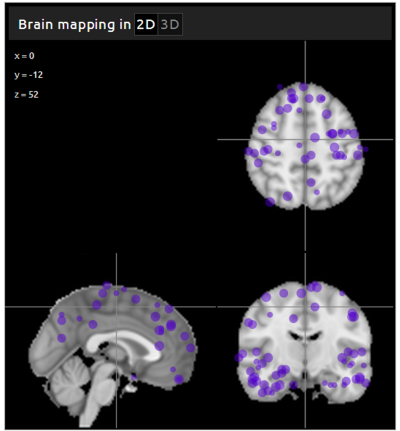
Brain mapping in 2D 3D
x = 0
y = -12
z = 52

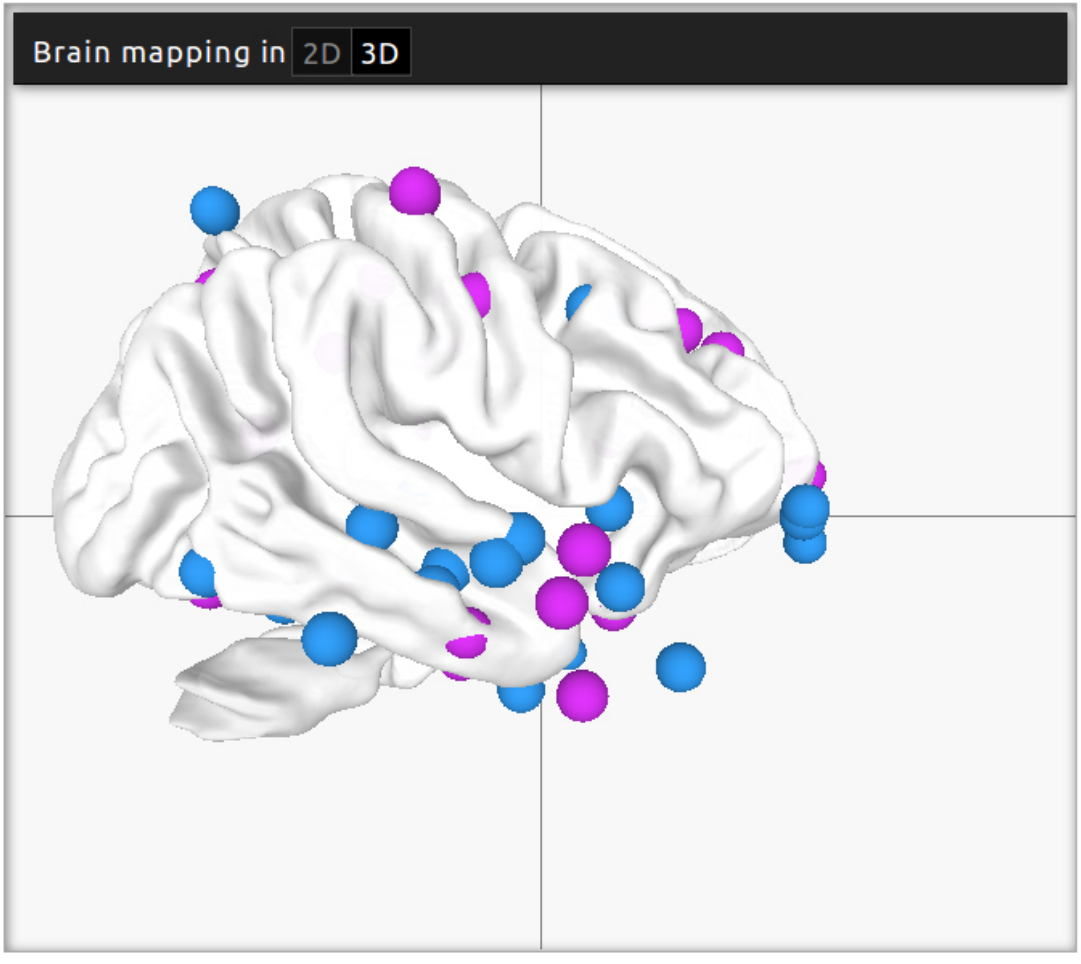
Brain mapping in 2D 3D

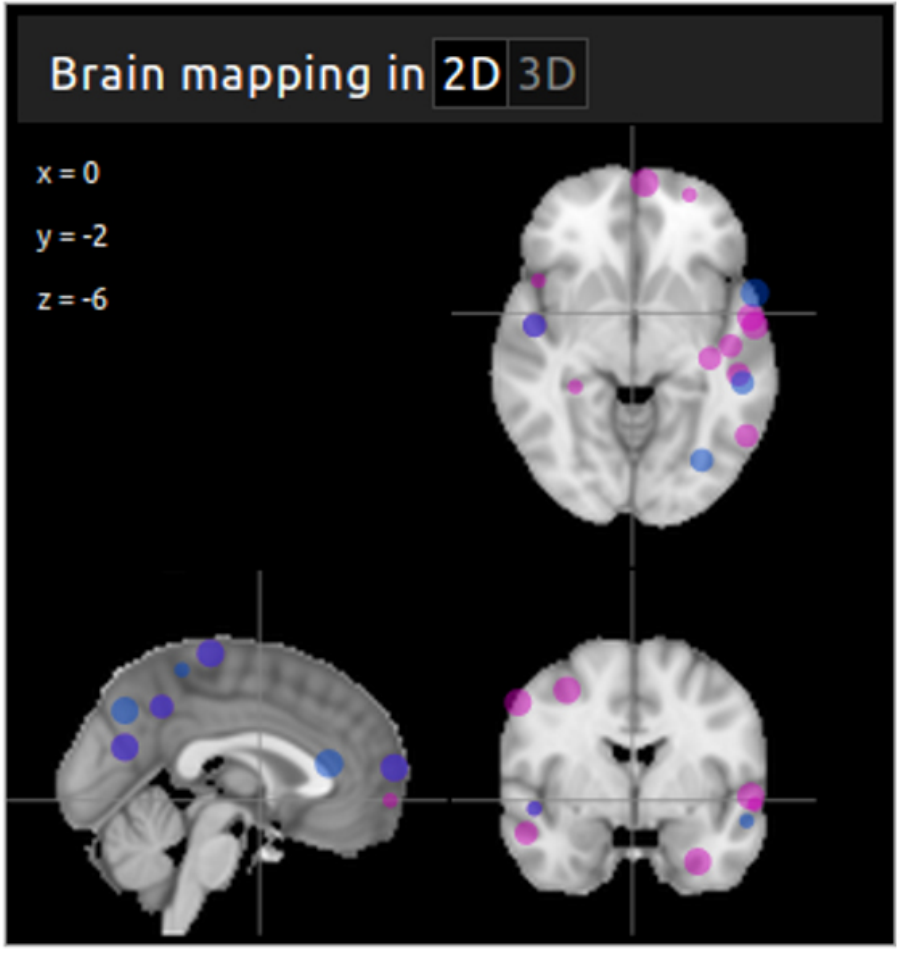
Brain mapping in 2D 3D
x = 0
y = -2
z = -6

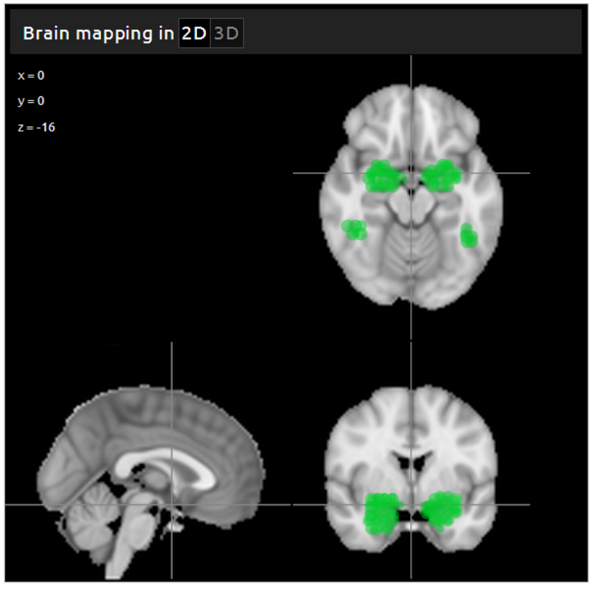
Brain mapping in 2D 3D
x = 0
y = 0
z = -16

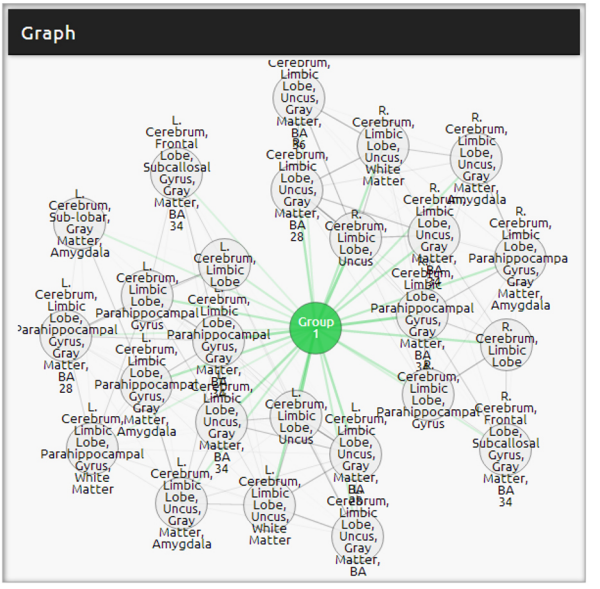
Graph
Group 1
L. Cerebrum, Frontal Lobe, Subcallosal Gyrus, Gray Matter, BA 34
L. Cerebrum, Sub-lobar, Gray Matter, Amygdala
L. Cerebrum, Limbic Lobe, Parahippocampal Gyrus, Gray Matter, BA 28
L. Cerebrum, Limbic Lobe, Parahippocampal Gyrus, White Matter
L. Cerebrum, Limbic Lobe, Uncus, Gray Matter, Amygdala
L. Cerebrum, Limbic Lobe, Uncus, White Matter
L. Cerebrum, Limbic Lobe, Uncus, Gray Matter, BA 34
L. Cerebrum, Limbic Lobe, Uncus, Gray Matter, BA
L. Cerebrum, Limbic Lobe, Uncus
L. Cerebrum, Limbic Lobe, Parahippocampal Gyrus, Gray Matter, BA 28
L. Cerebrum, Limbic Lobe, Parahippocampal Gyrus, Gray Matter, Amygdala
L. Cerebrum, Limbic Lobe, Parahippocampal Gyrus, Gray Matter, BA 34
L. Cerebrum, Limbic Lobe, Parahippocampal Gyrus, Gray Matter, BA
L. Cerebrum, Limbic Lobe, Parahippocampal Gyrus, Gray Matter, BA 34
L. Cerebrum, Limbic Lobe, Parahippocampal Gyrus, Gray Matter, BA
L. Cerebrum, Limbic Lobe, Parahippocampal Gyrus, Gray Matter, BA 34
L. Cerebrum, Limbic Lobe, Uncus, Gray Matter, BA 34
L. Cerebrum, Limbic Lobe, Uncus, Gray Matter, BA
L. Cerebrum, Limbic Lobe, Uncus, White Matter
L. Cerebrum, Limbic Lobe, Uncus, Gray Matter, BA
L. Cerebrum, Limbic Lobe, Uncus
L. Cerebrum, Limbic Lobe, Uncus, Gray Matter, BA 34
L. Cerebrum, Limbic Lobe, Uncus, Gray Matter, Amygdala
L. Cerebrum, Limbic Lobe, Uncus, White Matter
L. Cerebrum, Limbic Lobe, Uncus, Gray Matter, BA
R. Cerebrum, Limbic Lobe, Uncus, White Matter
R. Cerebrum, Limbic Lobe, Uncus, Gray Matter, Amygdala
R. Cerebrum, Limbic Lobe, Uncus, Gray Matter, BA 28
R. Cerebrum, Limbic Lobe, Uncus
R. Cerebrum, Limbic Lobe, Parahippocampal Gyrus, Gray Matter, Amygdala
R. Cerebrum, Limbic Lobe, Parahippocampal Gyrus, Gray Matter, BA 34
R. Cerebrum, Limbic Lobe, Parahippocampal Gyrus, Gray Matter, BA
R. Cerebrum, Limbic Lobe, Parahippocampal Gyrus
R. Cerebrum, Limbic Lobe
R. Cerebrum, Frontal Lobe, Subcallosal Gyrus, Gray Matter, BA 34

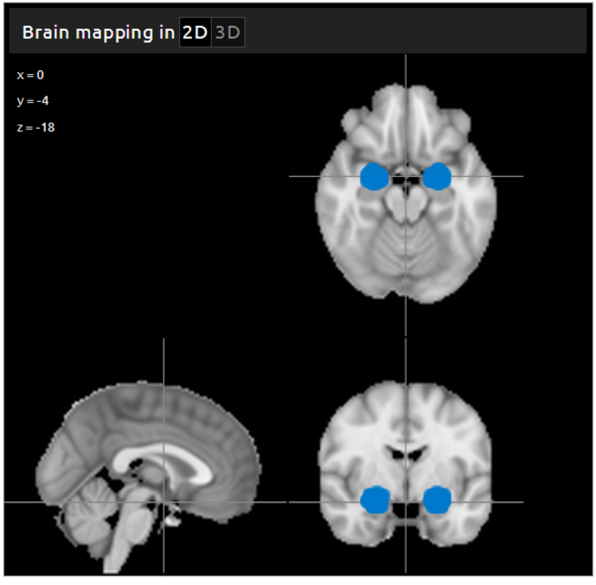
Brain mapping in 2D 3D
x = 0
y = -4
z = -18

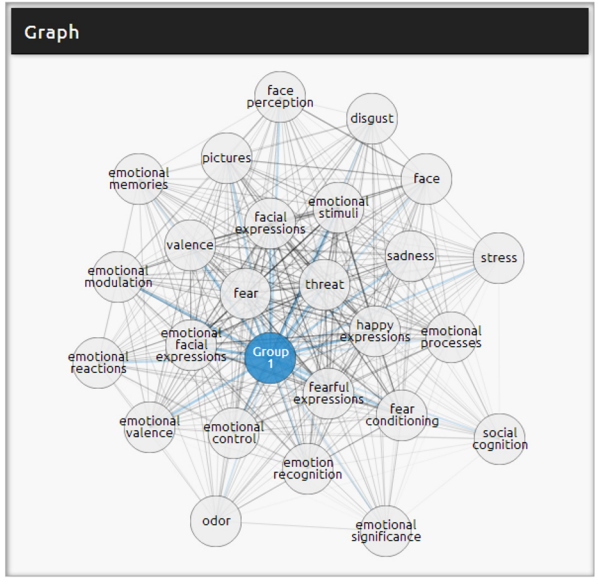
Graph
face perception
disgust
pictures
face
emotional memories
emotional stimuli
facial expressions
valence
sadness
stress
emotional modulation
fear
threat
happy expressions
emotional processes
Group 1
emotional facial expressions
emotional reactions
fearful expressions
fear conditioning
emotional valence
emotional control
social cognition
emotion recognition
odor
emotional significance


Graph

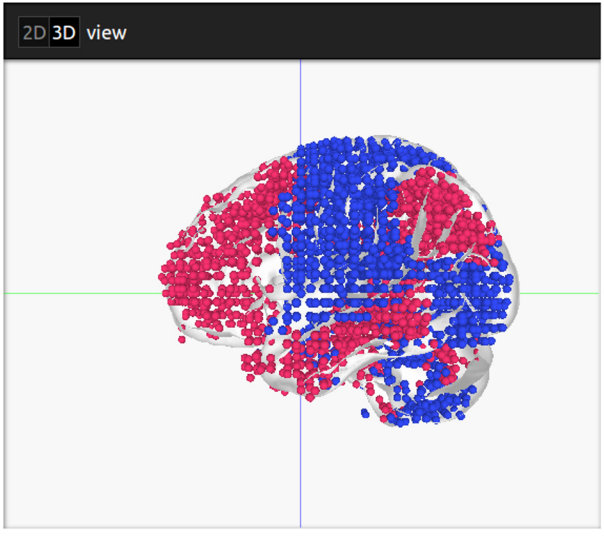
2D 3D view

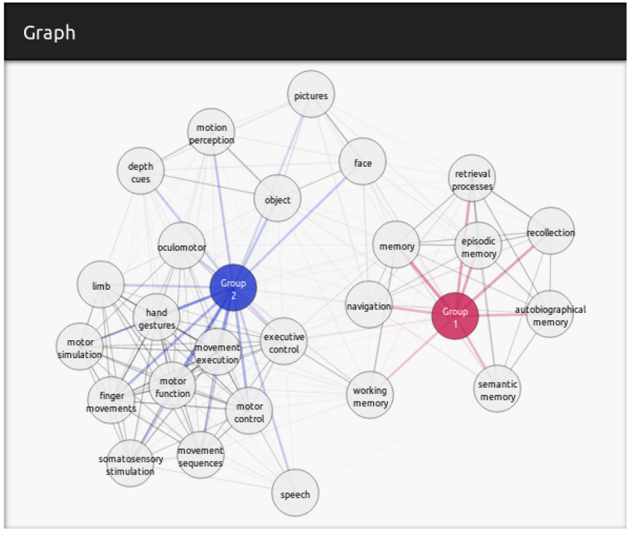
Graph
pictures
motion perception
face
depth cues
object
retrieval processes
memory
episodic memory
recollection
oculomotor
limb
Group 2
hand gestures
navigation
Group 1
autobiographical memory
motor simulation
executive control
movement execution
motor function
working memory
semantic memory
finger movements
motor control
somatosensory stimulation
movement sequences
speech

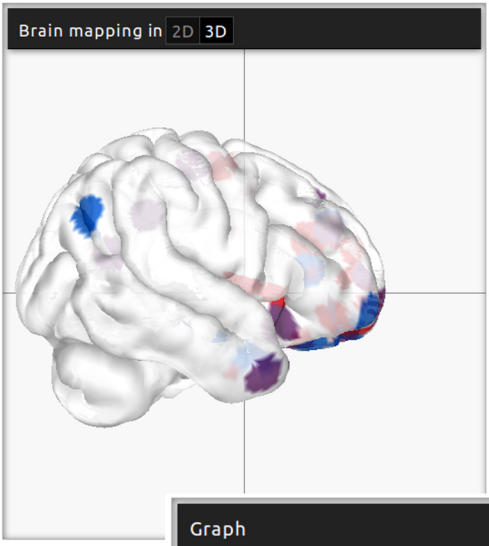
Brain mapping in 2D 3D

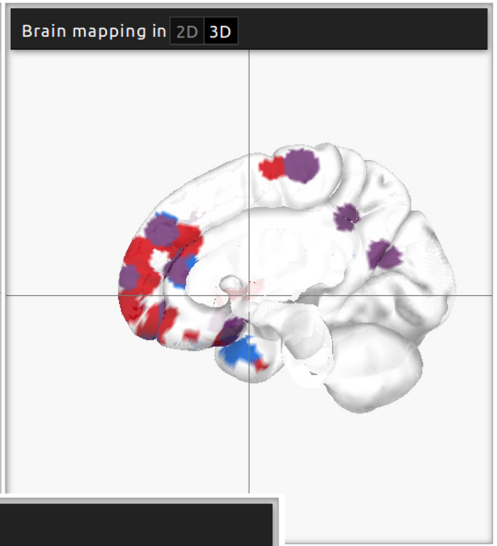
Brain mapping in 2D 3D

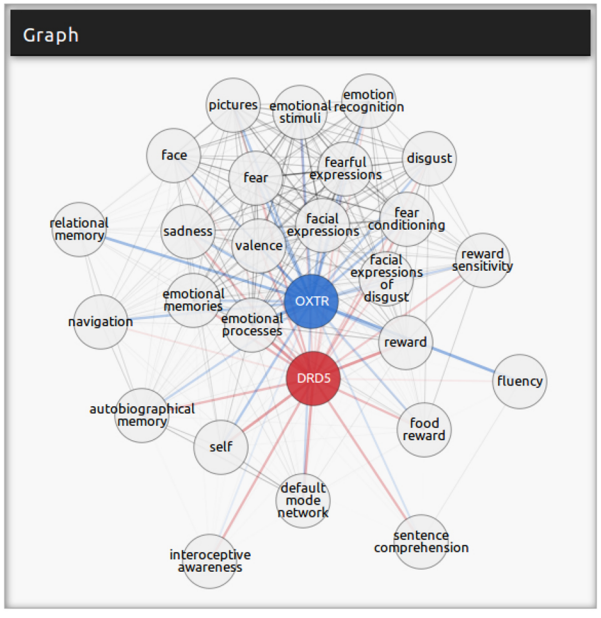
Graph
pictures
emotional stimuli
emotion recognition
face
fear
fearful expressions
disgust
relational memory
sadness
valence
facial expressions
fear conditioning
reward sensitivity
facial expressions of disgust
OXTR
emotional memories
navigation
emotional processes
reward
DRD5
fluency
autobiographical memory
self
food reward
default mode network
sentence comprehension
interoceptive awareness

Brain mapping in 2D 3D

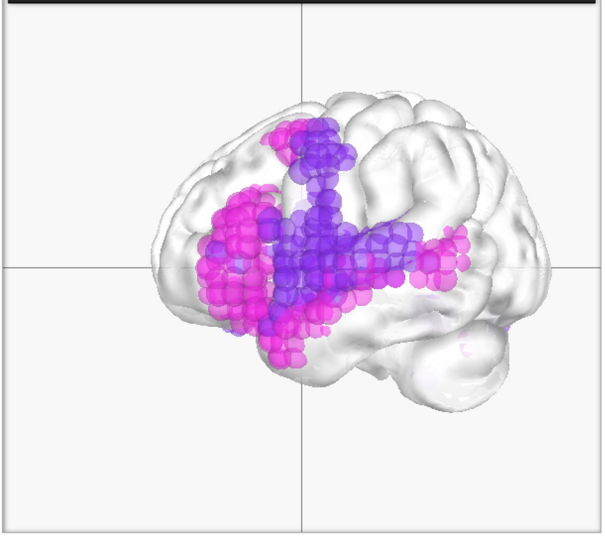

Graph

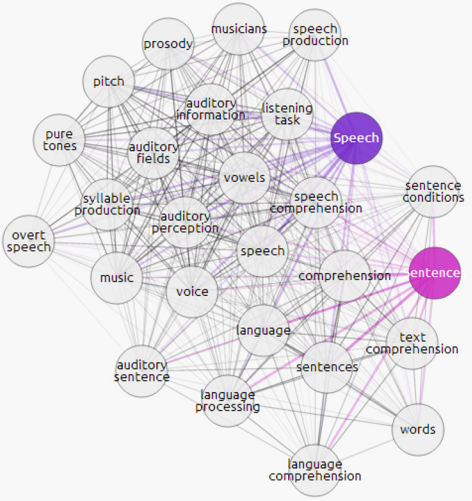

Graph

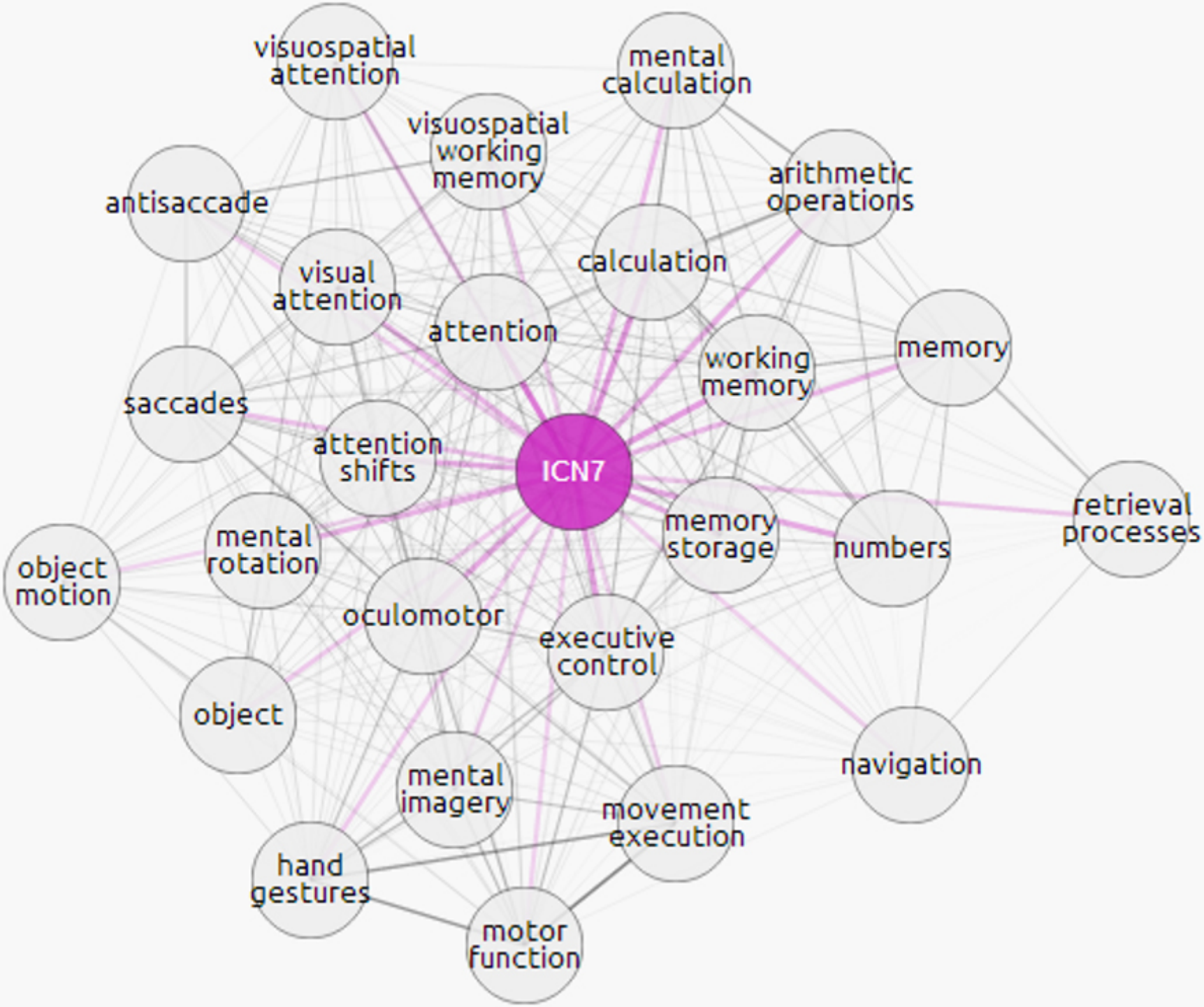
visuospatial attention
mental calculation
visuospatial working memory
antisaccade
arithmetic operations
visual attention
calculation
attention
memory
working memory
saccades
attention shifts
ICN7
retrieval processes
memory storage
numbers
mental rotation
object motion
oculomotor
executive control
object
navigation
mental imagery
movement execution
hand gestures
motor function